FIGURE S1

Related to Figure 1

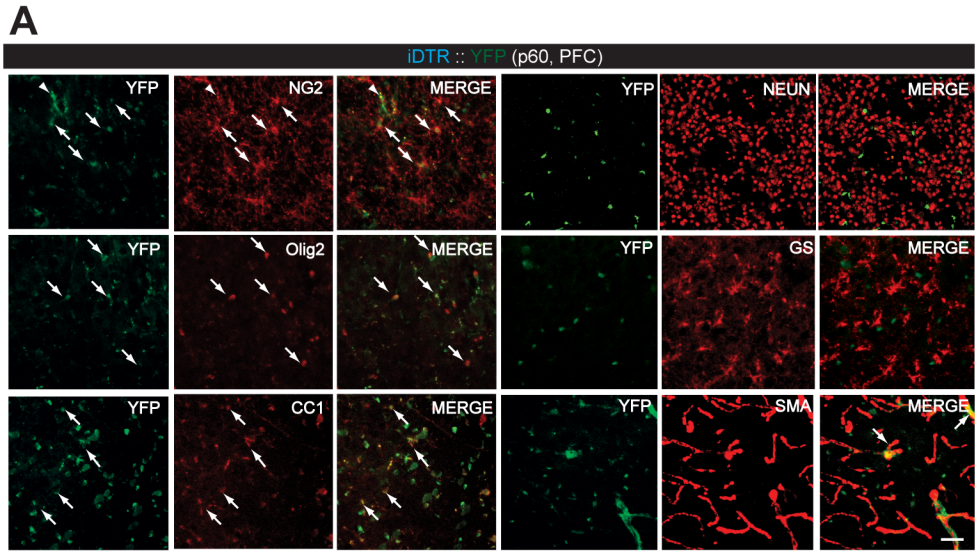

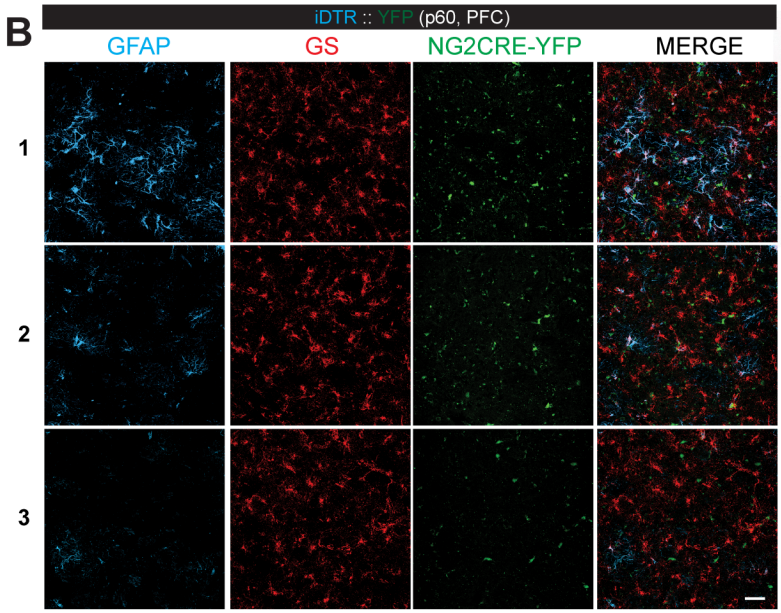

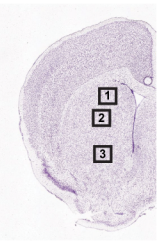

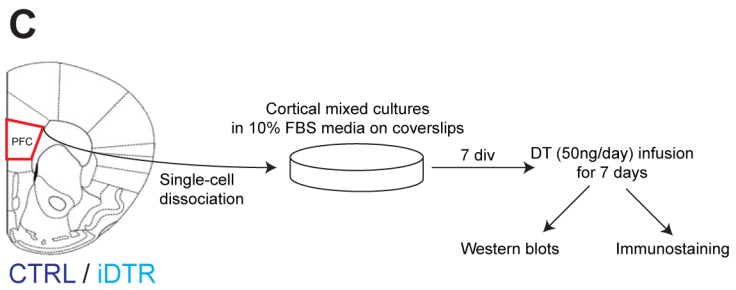

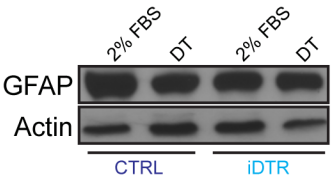

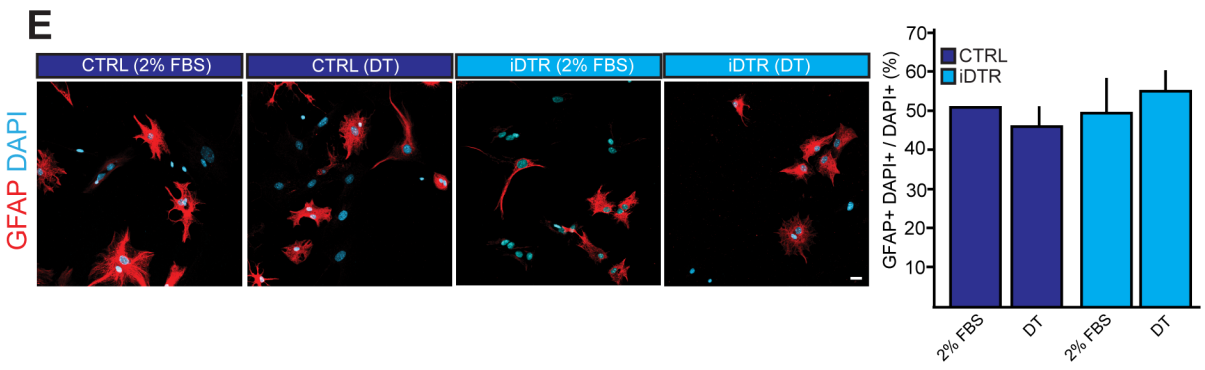

FIGURE S2
Related to Figure 1

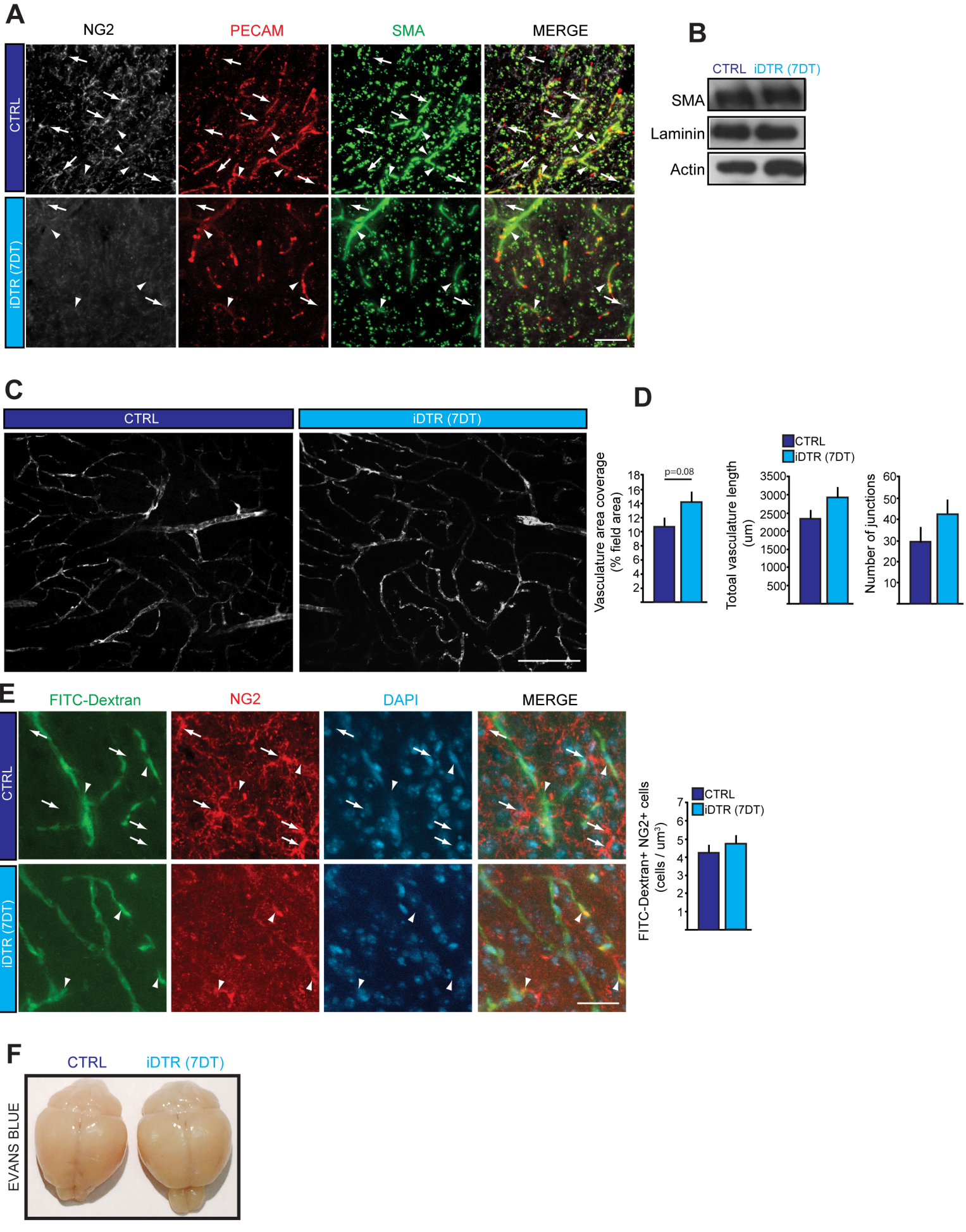

FIGURE S3
Related to Figure 1

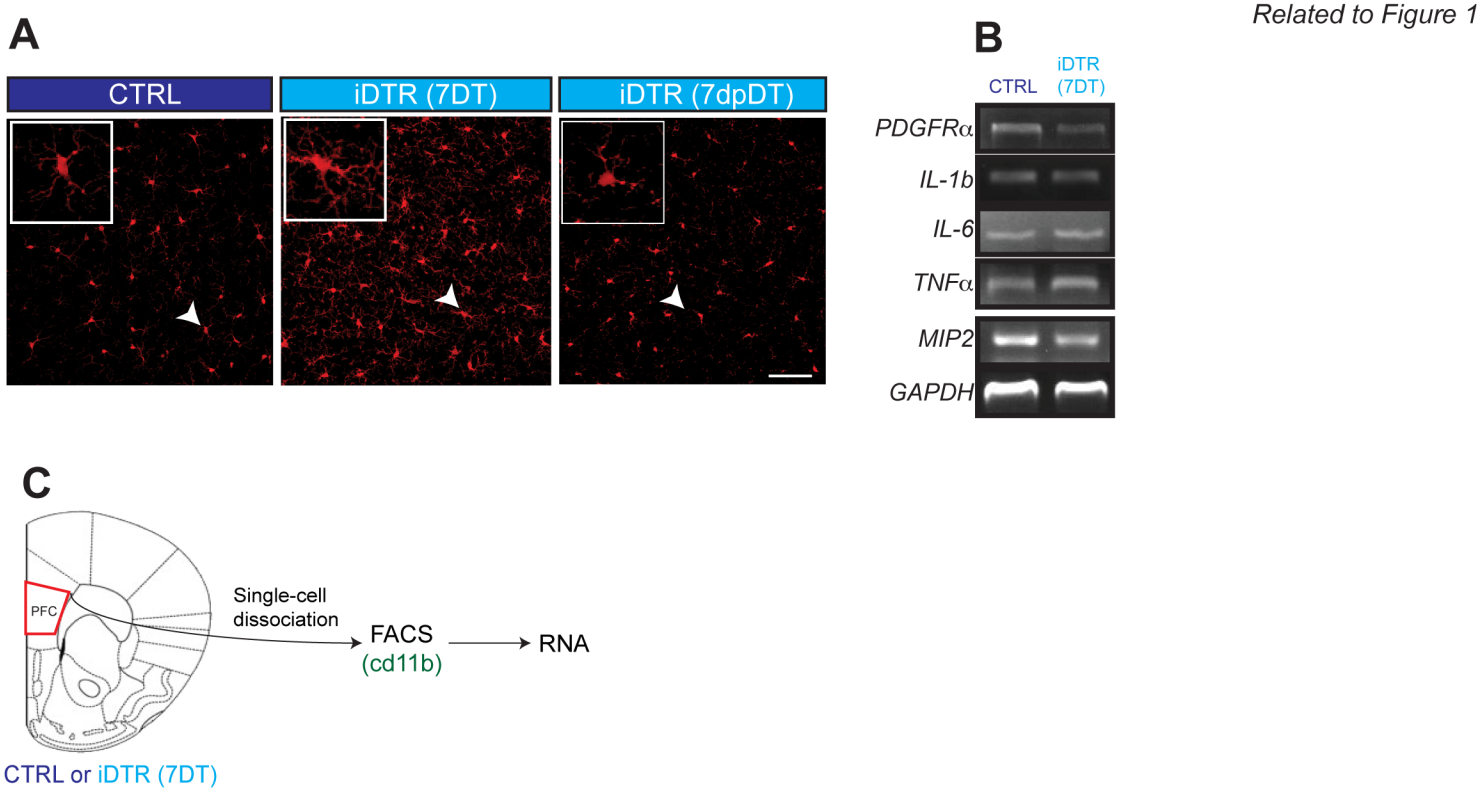

FIGURE S4
Related to Figure 2

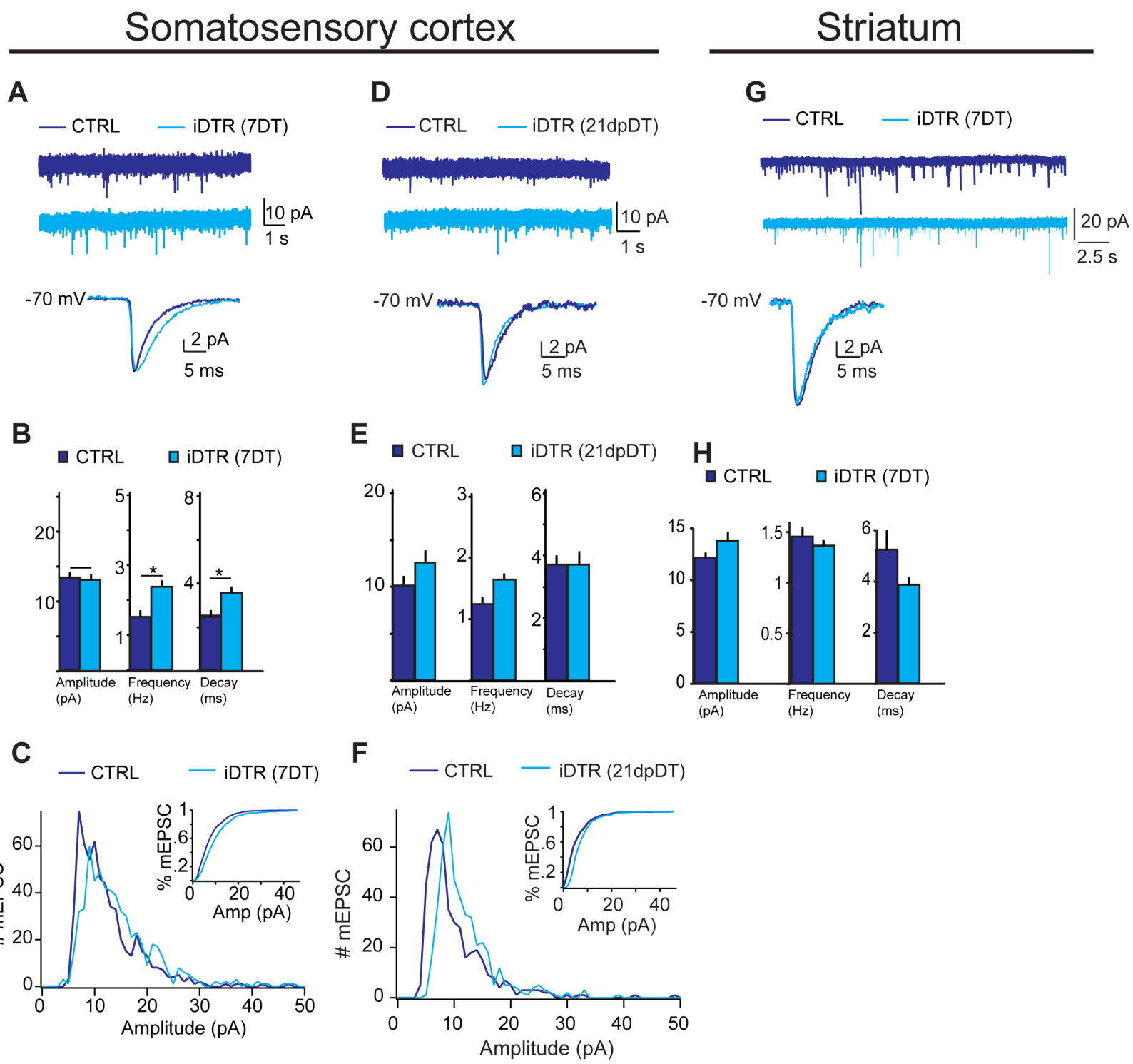

FIGURE S5
Related to Figure 4

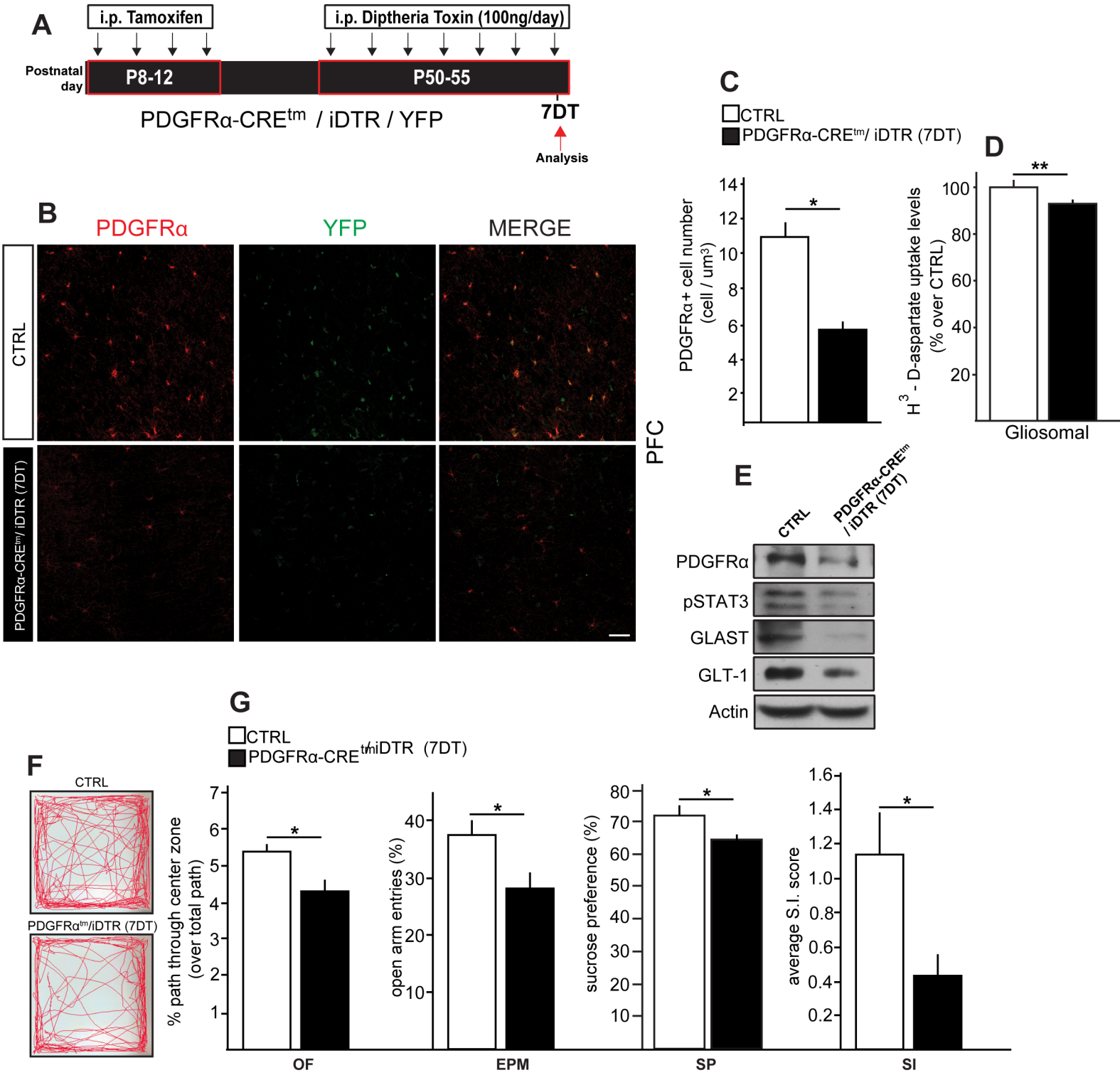

FIGURE S6
Related to Figure 8

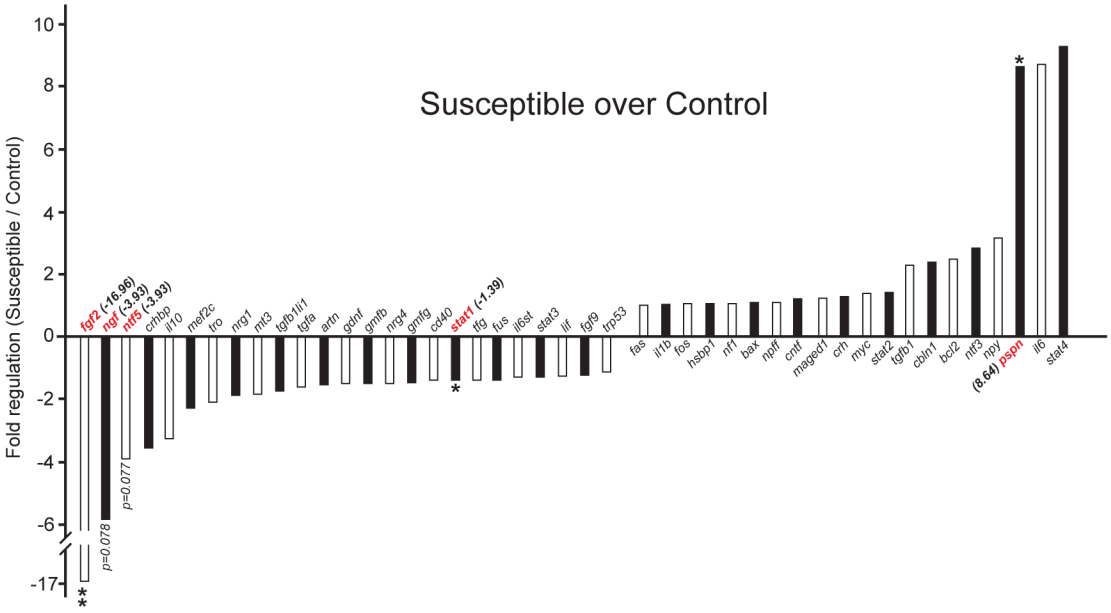

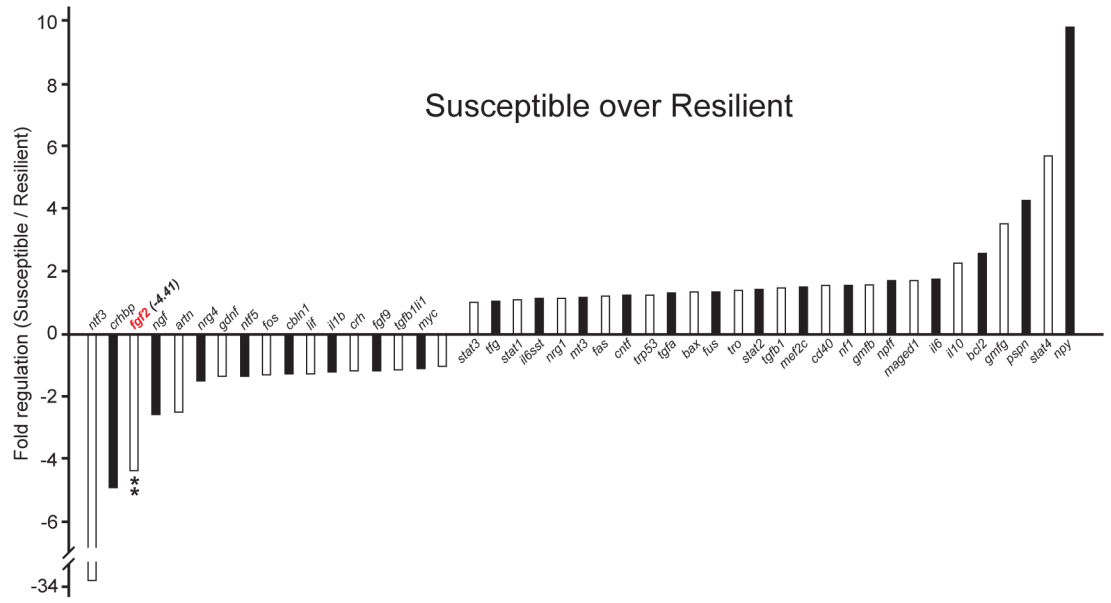

FIGURE S7

Related to Figure 8

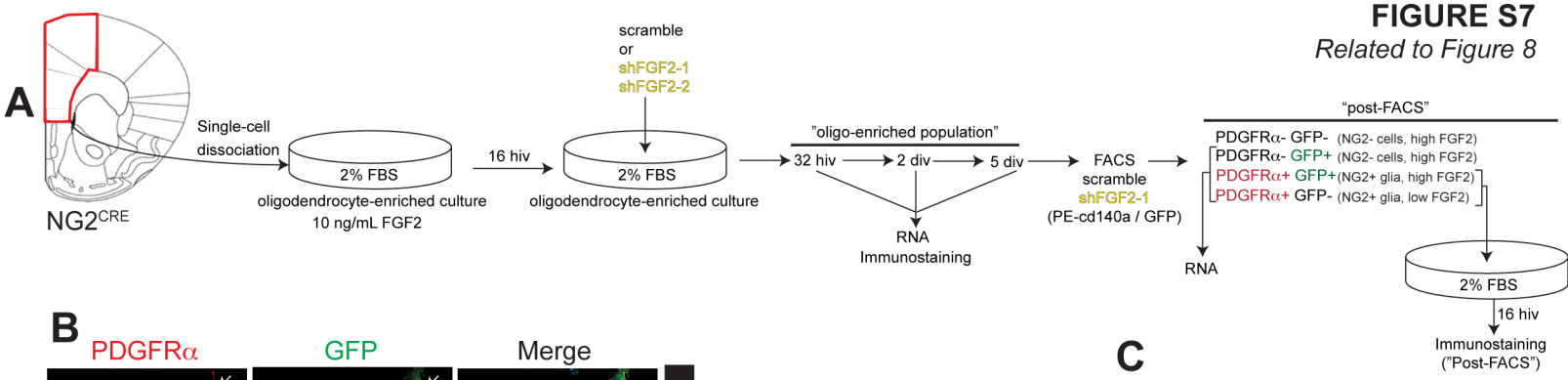

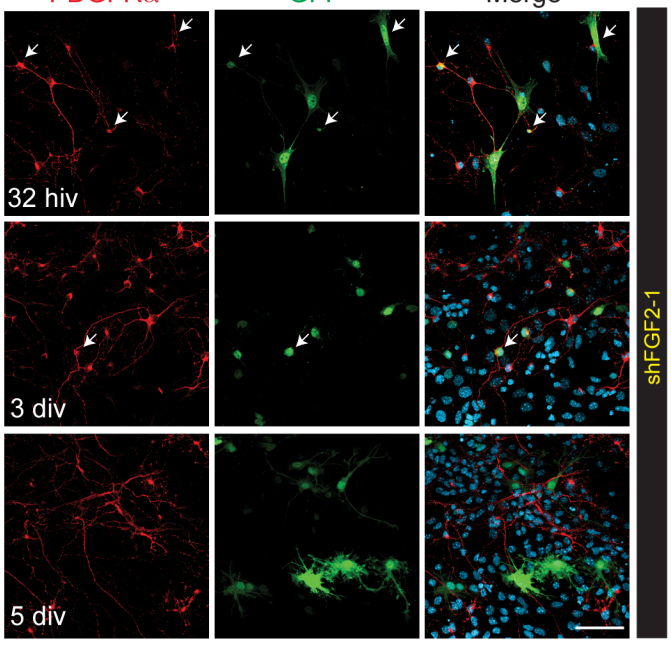

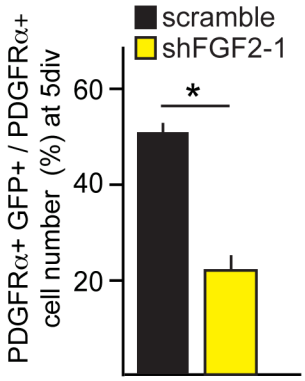

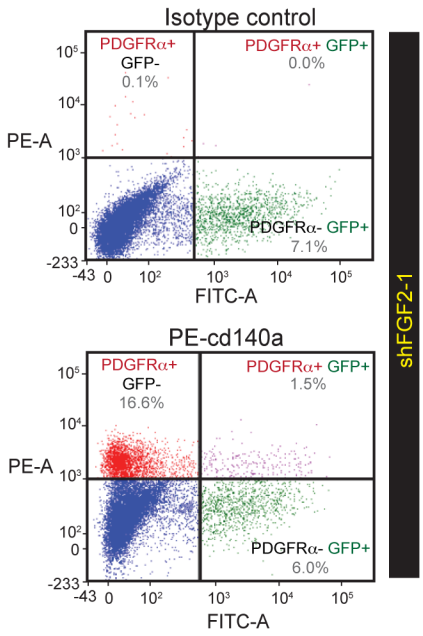

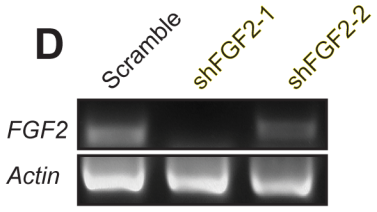

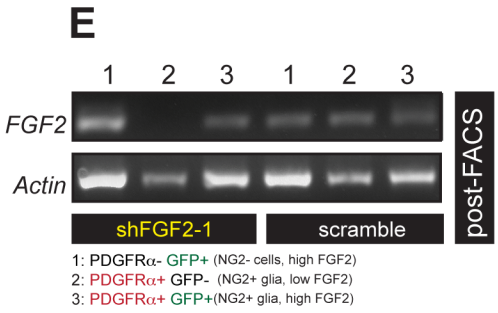

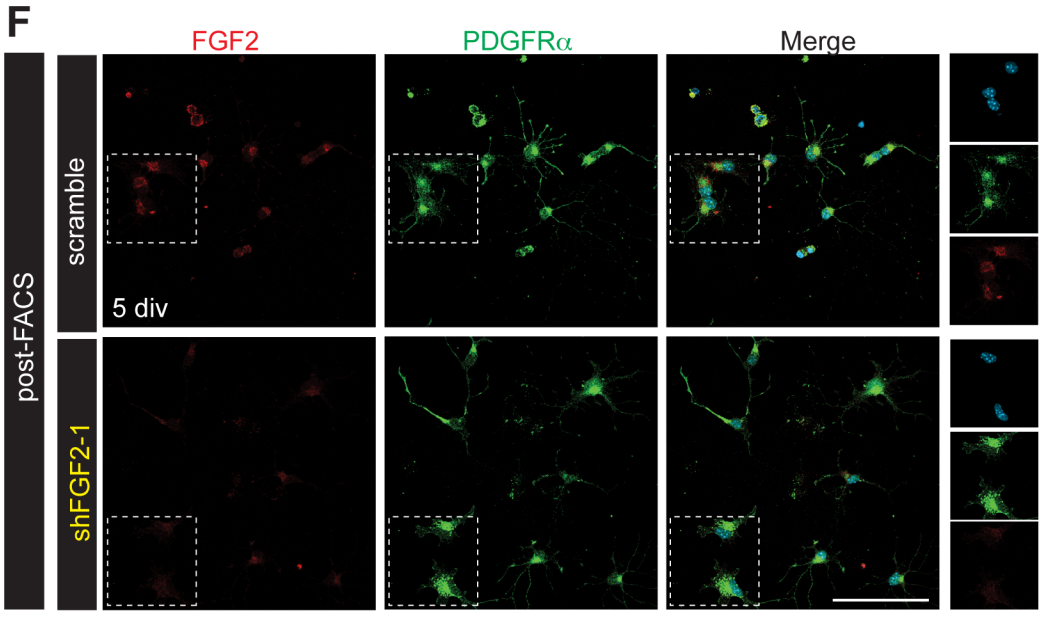

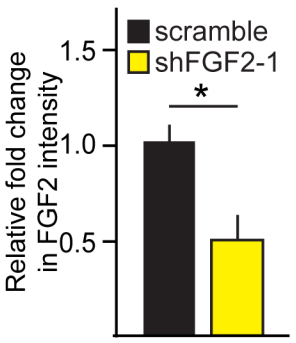

FIGURE S8

Related to Figures 1-8

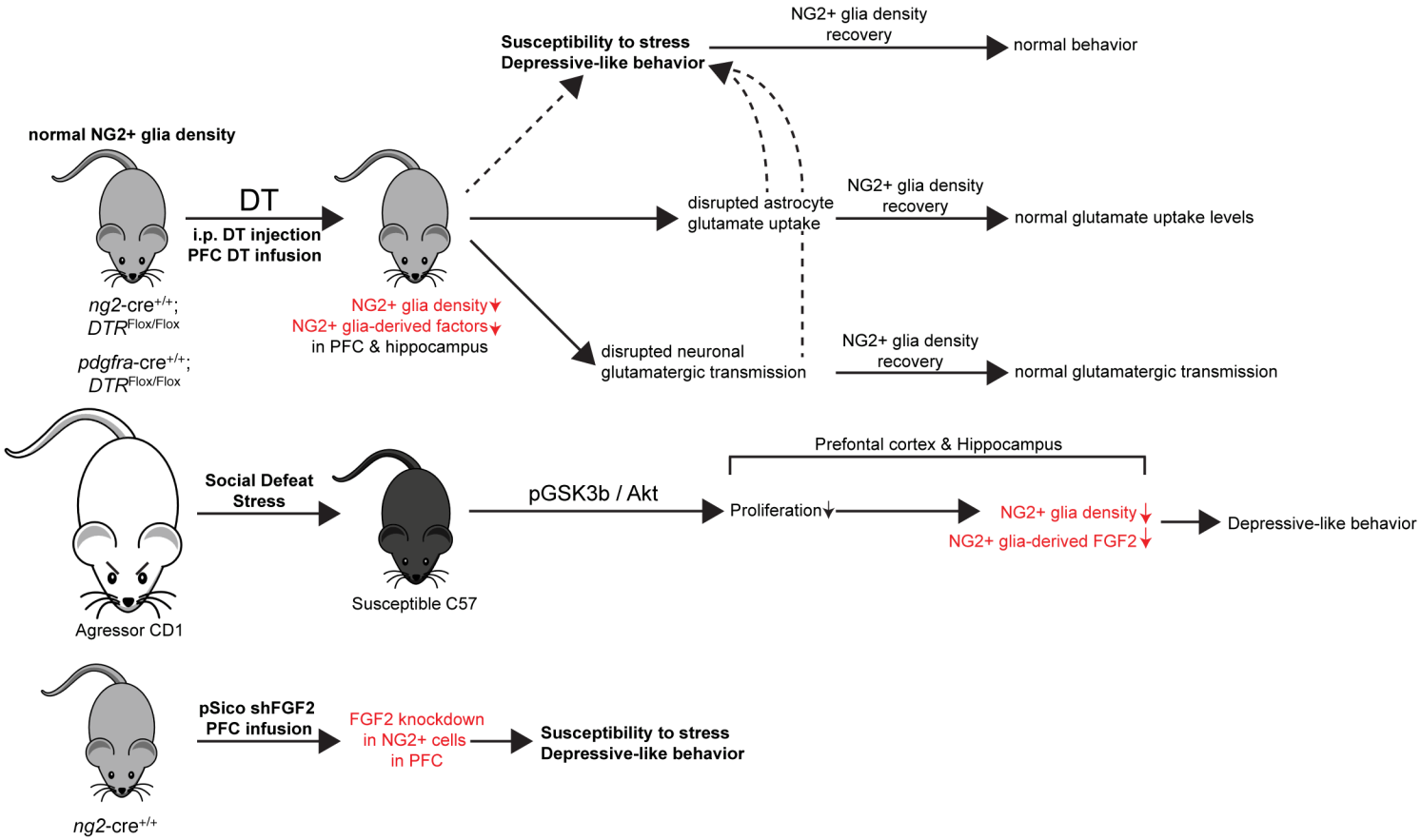

Supplemental Figure Legends

Figure S1 – Related to Figure 1.

Astrocytes do not express CRE and are not affected by DT administration. (**A**) Characterization of YFP+ cells in the adult PFC showed that the majority of this population co-localizes with the NG2 and Olig2 markers. A small number of YFP+ cells co-expressing the mature markers for oligodendrocytes (CC1+ cells) and pericytes (SMA+ cells) were observed in the PFC. YFP+ cells in the PFC of the NG2CRE/iDTR mouse do not co-localize with astrocytic markers, such as s100b, GFAP and glutamine synthase (red) neither in the PFC (**A**), nor in the striatum (**B**). Right, numbered boxes indicate striatal regions examined. **(C)** Schematic represent the method used for the isolating and analysis of primary astrocytes from the cortices of NG2CRE/iDTR mice following DT infusion. Primary astrocyte cultures obtained from adult NG2CRE/iDTR PFCs were treated for 7 days with DT and then processed to detect total GFAP protein levels **(D)** and cell quantification GFAP+ cells (astrocytes) using immunocytochemistry analysis **(E)**. Error bars represent mean ± SEM. Scale Bar; 40μm. n=4 per group.

Figure S2 – Related to Figure 1.

CNS vasculature and blood-brain-barrier are not perturbed during NG2 glia ablation. (A and B) To rule out effects on pericytes (known to express the NG2 proteoglycan) and on possible blood-brain-barrier (BBB) and vascular perturbations during the DT administration, we characterized pericytes and endothelial cells in the PFCs of control and iDTR at 7DT with conventional cellular markers to identify these populations. At 7DT, NG2 glia (arrowheads) were ablated, while pericytes (arrows; PCAM+ cells and SMA+ cells) were preserved in the PFC. (**C**) CNS microvasculature integrity was monitored by intracardiac injection of FITC-conjugated dextran sulfate. **(D)** Vasculature integrity was quantified by area coverage, total vessel length and number of branch point **(E)** Representative images of NG2 (red), FITC-dextran (green) and DAPI (blue) at 7DT. . Arrows indicate NG2 glia and arrowheads indicate NG2+ pericytes. **(F)** Evans blue dye injections were used to monitor BBB integrity during NG2 glial ablation. Evans blue assay in the iDTR mice at 7DT showed no vascular leakage at this or anytime postDT treatment, suggesting preserved BBB integrity. Error bars represent mean ± SEM. Scale bars: (A) 40μm (C) 100μm (D) 20μm.

Figure S3 – Related to Figure 1.

NG2 glia ablation does not cause inflammation or microglial activation. (A) Representative images of microglia (Iba-1+ cells) in the PFC of control and iDTR mice at 7DT and 7dpDT. **(B)** Gene expression levels of pro-inflammatory cytokines in the PFC and control and iDTR mice at 7DT. **(C)** Isolation of microglia from the PFCs of CTRL and iDTR at 7DT. **(D)** Representative plots of FACS gates used to isolate microglia (cd11b+ cells). **(E)** Similar levels of pro-inflammatory cytokines were observed in isolated cd11b+ cells between control or iDTR mice at 7DT. Scale Bar; 40μm

Figure S4 – Related to Figure 2.

Glutamatergic transmission in the somatosensory cortex at 7DT and 21dpDT and striatum. (A) Representative traces of mEPSC recordings from layer 2/3 somatosensory pyramidal neurons in control and iDTR mice at 7DT (Control: n = 18; DTR: n = 23). Top: raw traces. Bottom: average mEPSC. **(B)** Plot of average amplitude (Amp), Frequency (Freq), and decay time constant. **(C)** Histogram (panel) and cumulative distribution (inset) of mEPSC amplitude. **(D)** Representative traces of mEPSC recorded from Layer 2/3 pyramidal neurons in control and iDTR at 21dpDT (Control: n=10; 21dpDT: n=6). Top: raw traces for Control and iDTR. Bottom: average mEPSC. **(E)** Average amplitude (Amp), Frequency (Freq) and decay time constant (Decay) for Control and iDTR at 21dpDT. (F) Histogram (panel) and cumulative distribution (inset) of mEPSC amplitudes from Control and iDTR at 21dpDT. **(G)** Representative traces of mEPSC recordings from the striatal neurons in control and iDTR mice at 7DT (Control: n = 18; DTR: n = 23). Top: raw traces. Bottom: average mEPSC. (H) Plot of average amplitude (Amp), Frequency (Freq), and decay time constant. Error bars represent mean ± SEM. (*P < 0.05; t-test)

Figure S5 – Related to Figure 4.

NG2 glial cell ablation in the PDGFRα^{CRETM}/iDTR/YFP mouse line parallel the deficits observed in the NG2^{CRE}/iDTR mouse line. **(A)** Experimental paradigm for depletion of NG2 glia in the PFC of the PDGFRα^{CREtm}/iDTR/YFP mice. PDGFRαCREtm/iDTR/YFP mice at postnatal day 8 (P8) received tamoxifen injection once daily for 4 consecutive days and 45 days later the DT was injected. Representative images **(B)** and cell number **(C)** of NG2 glia (PDGFRα+ cells) in the PFC of the PDGFRαCREtm/iDTR/YFP and control mice at 7DT. (n=5 per group). **(D)** 3H-D-aspartate uptake assayed from PFC gliosomes of control and PDGFRαCREtm/iDTR/YFP mice at 7DT (n=8 per group). **(E)** Protein expression levels of PDGFRα, pSTAT3, pPKC, GLAST, GLT-1 and actin from PFC of control and PDGFRαCREtm/iDTR/YFP mice at 7DT. (**F-G**) Behavioral analyses animals at 7DT (n=17-21 per group). **(F)** Open field activity and % center entry frequencies over general activity. **(G)** % in open arm entry frequencies over all entries number analyzed by Elevated Plus Maze test, 1% sucrose consumption preference (SP) and Social interaction of control and PDGFRαCREtm/iDTR/YFP mice at 7DT. Average Social Interaction (S.I.) scores following microdefeat. (n=10-11 per group) Error bars represent mean ± SEM. (*p<0.05; **p<0.01; t-test). Scale bar: 40μm.

Figure S6 – Related to Figure 8.

Differential transcriptional profiles of NG2 glia-expressed cue factors during social defeat. Selected genes in red represent hits that are significant or trending towards significant change during social defeat; Right, Fold changes of differentially regulated genes in Susceptible PFC over Control PFC, Left, Susceptible over Resilient, Bottom, Susceptible over Resilient. Numbers in parentheses represent the fold regulation. See Table 2 for the annotation information for selected genes.

Figure S7 – Related to Figure 8.

***In vitro* validation of the shRNA strategy using lentiviral cre/flox system to knockdown FGF2 specifically in NG2 glial cells. (A)** Experimental design for the *in vitro* validation of lentivirus-mediated, CRE-dependent knockdown of mouse FGF2 in NG2 cells. Brain cortices of adult NG2CRE mice were isolated, cultured in oligodendrocyte progenitor-enriching conditions and infected with either of the lentiviral constructs (LVs) shFGF2-1, shFGF2-2 or scramble control. The culture were then either processed for FAC-sorting of LV-targeted NG2 cells to obtain RNA and detect mouse *FGF2* mRNA levels and immunocytochemistry analysis to detect FGF2 levels. **(B)** Cortical cell cultures from NG2CRE cortices were processed at different time-points to detect LV transduction efficiency in a CRE-dependent loss of GFP reporter in PDGFRα+ cells. **(C)** Typical FACS profiles for cell populations isolated (see panel A, far right) from infected cultures with shFGF2-1. **(D)** PCR analysis of isolated PDGFRα+GFP^{neg} cells at 5dpi with shFGF2-1 or scramble. The LV shFGF2-1 construct achieved the highest knockdown of mouse mRNA *FGF2* in NG2 glial cells as compared with scramble and shFGF2-2. **(E)** Mouse *FGF2* mRNA levels of cell populations post-FACS from shFGF2-1 and scramble infection conditions. **(F)** Relative FGF2 fluorescence levels between scramble and shFGF2-1 infected PDGFRα+ cells post-FACS. Error bars represent mean ± SEM. hiv= hours in vitro; div= days in vitro. n=4 per group. Scale bars: 40μm.

Figure S8 - Related to Figures 1-8. Working model

Chronic social stress reduces NG2 glial cell proliferation capacity and density via decreasing the phosphorylation state of GSK3β in NG2 glia. The FGF2 cue was identified as a possible NG2 glia-derived factor, whose loss might be upstream of other stress-associated dysfunctions in astrocytes and neurons. NG2 glia loss was simulated in stress-naïve mice by using Diphtheria Toxin-mediated cell ablation system. This was able to recreate functional deficits in astrocytes and neurons, in glutamate uptake and glutamatergic signaling respectively, which have previously been implicated in the pathophysiology of MDD. The recovery of NG2+ glia cell density rescued all of the molecular, cellular and behavioral deficits observed acutely after NG2+ glia ablation.

.

Supplemental Tables

TABLE 1 : Patient information for the post-mortem tissue samples used in the study
NICHD BRAIN AND TISSUE BANK FOR DEVELOPMENTAL DISORDERS (MARYLAND)

Sample	Disorder	Diagnosis	Cause of Death	Medications	Age	Gender	PMI	AD
5239	Depression,NOS	Depression, Drug Abuse	Methadone intox.	Methadone, Clonipine	21	Male	4	Y
4916	Control	n/a	Accident, Drowning	None	19	Male	5	N
5122	Depression,NOS	Depression, Drug Abuse, Alcohol Abuse, Smoker	Narcotic & Ethanol intox	Lexapro	35	Male	19	Y
5398	Control	Burns: Right Hand, Abdomen, Left Foot	Electrocution	None	36	Male	24	N
1551	Depression,NOS	Depression, Cardiac Arrest	Multiple Injuries-accident	Zoloft	43	Female	23	Y
4841	Control	Slight Hypertension	Multiple Injuries-accident	None	42	Female	17	N
1454	Depression,NOS	Depression, Drug overdose	Combined Drug Intox	Seroquel, Clonazepan, Remeron, Celexa	47	Female	24	Y
5347	Control	Mild Hypertension, Syncopal episodes	Cardiac Arrythmia	None	46	Female	9	N
5245	Depression,NOS	Depression, Drug Abuse, Alcohol Abuse, Smoker	Oxycodone Toxicity	None	23	Male	24	N
5175	Depression,NOS	Depression, Drug Abuse, Alcohol Abuse, Smoker	HCVD complicated by cocaine use	None	47	Male	22	N
1611	Depression,NOS	Depression	Suicide, Hanging	None	18	Male	11	N
4919	Depression,NOS	Depression	Suicide, Hanging	None	21	Female	25	N

HUMAN BRAIN AND SPINAL FLUID RESOURCE CENTER (CALIFORNIA)

Sample	Disorder	Diagnosis	Cause of Death	Medications	Age	Gender	PMI	AD
567	Depression	Major Depression, Alcohol Abuse	Suicide-overdose	Digoxin, Lasix, Pronestyl, Dalmane	79	Male	26.5	Y
600	Depression	Major Depression, Alcohol Abuse, Hypertension	n/a	N/A	37	Male	33	N/A
510	Depression	Major Depression, Alcohol Abuse, Siezure Disorder	Food Aspiration	Dilantin; Serantil; Valium	50	Male	45	Y
529	Depression	Major Depression	Drug Overdose	Phenothiazines, Amitriptyline, Nortriptyline	48	Female	24	Y
3504	Control	Cancer-renal, Hypertension	CA-complications	Duragesic Patch	80	Male	11	N
3529	Control	Cancer-colon	CA-complications	Glucovance,Cartia-XT	58	Male	9	N
3535	Control	Lymphoma-non-hodgkins	Lymphoma-complications	Phentoin , Morphine Lorazepam, Diazepam	81	Male	14	Y
3540	Control	Cancer-lung, Alcohol abuse, Diabetes Type k	CA-complications	Coumadin, Digoxin, Insulin	68	Male	10.5	N

Table 1 (Related to Figure 6)

Patient information for the post-mortem tissue samples used in the study

Detailed patient information of post-mortem MDD investigated in the study. Samples were obtained from two independent tissue banks, NICHD Brain and Tissue Bank for Developmental Disorders and Human Brain and Spinal Cord Center. Age, gender, diagnosis, cause of death, available medication history and post-mortem interval (PMI) are provided. AD=Antidepressant use

TABLE 2: Gene information for selected neurotrophins assessed by PCR array

Unigene	Refseq	Symbol	Description	RT2 Catalog
Mm.56897	NM_009711	*Artn*	Artemin	PPM04308C
Mm.19904	NM_007527	*Bax*	Bcl2-associated X protein	PPM02917E
Mm.257460	NM_009741	*Bcl2*	B-cell leukemia/lymphoma 2	PPM02918F
Mm.4880	NM_019626	*Cbln1*	Cerebellin 1 precursor protein	PPM04309F
Mm.271833	NM_011611	*Cd40*	CD40 antigen	PPM03426C
Mm.290924	NM_170786	*Cntf*	Ciliary neurotrophic factor	PPM68695B
Mm.290689	NM_205769	*Crh*	Corticotropin releasing hormone	PPM04632A
Mm.316614	NM_198408	*Crhbp*	Corticotropin releasing hormone binding protein	PPM04311B
Mm.1626	NM_007987	*Fas*	Fas (TNF receptor superfamily member 6)	PPM03705B
Mm.473689	NM_008006	*Fgf2*	Fibroblast growth factor 2	PPM03040B
Mm.8846	NM_013518	*Fgf9*	Fibroblast growth factor 9	PPM02979F
Mm.246513	NM_010234	*Fos*	FBJ osteosarcoma oncogene	PPM02940C
Mm.277680	NM_139149	*Fus*	Fusion, derived from t(12;16) malignant liposarcoma (human)	PPM04620G
Mm.4679	NM_010275	*Gdnf*	Glial cell line derived neurotrophic factor	PPM04315F
Mm.87312	NM_022023	*Gmfb*	Glia maturation factor, beta	PPM04320C
Mm.194536	NM_022024	*Gmfg*	Glia maturation factor, gamma	PPM04619B
Mm.13849	NM_013560	*Hspb1*	Heat shock protein 1	PPM02936B
Mm.874	NM_010548	*Il10*	Interleukin 10	PPM03017C
Mm.222830	NM_008361	*Il1b*	Interleukin 1 beta	PPM03109F
Mm.1019	NM_031168	*Il6*	Interleukin 6	PPM03015A
Mm.4364	NM_010560	*Il6st*	Interleukin 6 signal transducer	PPM03123C
Mm.4964	NM_008501	*Lif*	Leukemia inhibitory factor	PPM02988F
Mm.27578	NM_019791	*Maged1*	Melanoma antigen, family D, 1	PPM04654E
Mm.451574	NM_025282	*Mef2c*	Myocyte enhancer factor 2C	PPM04548A
Mm.2064	NM_013603	*Mt3*	Metallothionein 3	PPM04012A
Mm.2444	NM_010849	*Myc*	Myelocytomatosis	PPM02924F

			oncogene	
Mm.488324	NM_010897	*Nf1*	Neurofibromatosis 1	PPM05038F
Mm.1259	NM_013609	*Ngf*	Nerve growth factor	PPM03596B
Mm.445915	NM_018787	*Npff*	Neuropeptide FF-amide peptide precursor	PPM04653A
Mm.154796	NM_023456	*Npy*	Neuropeptide Y	PPM04323A
Mm.460675	NM_178591	*Nrg1*	Neuregulin 1	PPM57587C
Mm.443874	NM_032002	*Nrg4*	Neuregulin 4	PPM04712B
Mm.267570	NM_008742	*Ntf3*	Neurotrophin 3	PPM04325A
Mm.20344	NM_198190	*Ntf5*	Neurotrophin 5	PPM04324A
Mm.86487	NM_008954	*Pspn*	Persephin	PPM04335A
Mm.487336	NM_009283	*Stat1*	Signal transducer and activator of transcription 1	PPM04025F
Mm.471333	NM_019963	*Stat2*	Signal transducer and activator of transcription 2	PPM04656C
Mm.249934	NM_011486	*Stat3*	Signal transducer and activator of transcription 3	PPM04643F
Mm.1550	NM_011487	*Stat4*	Signal transducer and activator of transcription 4	PPM04644B
Mm.489792	NM_019678	*Tfg*	Trk-fused gene	PPM34272F
Mm.137222	NM_031199	*Tgfa*	Transforming growth factor alpha	PPM03051G
Mm.248380	NM_011577	*Tgfb1*	Transforming growth factor, beta 1	PPM02991B
Mm.3248	NM_009365	*Tgfb1i1*	Transforming growth factor beta 1 induced transcript 1	PPM04439C
Mm.3597	NM_019548	*Tro*	Trophinin	PPM04339E
Mm.222	NM_011640	*Trp53*	Transformation related protein 53	PPM02931C

Table 2 (Related to Figure 8)

Gene information on selected neurotrophins from RT^2 PCR Array

ReqSeq annotations, descriptions, alternative names and RT2 catalog numbers of the genes represented in Fig. S8.

Supplemental Experimental Procedures

Immunohistochemistry. For PFC immunostaining, free floating coronal brain slices included anti-BrdU (Accurate), anti-NG2 (Chemicon, R&D systems), anti-GFAP (mouse monoclonal, Sigma Aldrich), anti-GFAP (Covance), anti-S100b (DAKO, rabbit anti-human clone A5110), anti-PDGFRα (BD Biosciences), anti-pGSK3b (Cell Signalling) anti-CC1 (Calbiochem), anti-Ki67 (Novocastra), anti-PCNA (Chemicon), anti-glutamine synthase (Abcam), anti-PECAM (Chemicon), anti-SMA (Dako), anti s100b, anti-GLAST (Abcam), anti-Iba-1 (Wako), and anti-Olig2 (Abcam). For newly generated cells, Bromodeoxyuridine (BrdU) was dissolved in drinking water (1mg/ml), and mice were given access to the water ad libitum for 3 weeks after 7DT. For BRDU staining, sections were incubated with 2N Hydrochloric acid (HCL) for 20 minutes at 37^{o}C and then washed with PBS for 30 minutes. For PCNA staining, sections were boiled in 0.1M sodium citrate, pH 4.5, in a water-steamer bath apparatus. For terminal deoxynucleotidyl transferase dUTP nick end labeling (TUNEL), we followed the manufacturer's instructions (In situ Cell Death Detection Kit, Roche). NG2 glia immunostaining from fresh-frozen brains, tissue sections (10um sections) were pre-treated with a 1:1 ethanol:methanol post-fixation treatment .

Western blots and immunoprecipitation. For western blots, the PFCs of the specified mouse strain or treatment group were dissected out at the end of the experiments and used for protein extraction using lysis buffer (50mM Tris-HCl, pH7.5, 1mMEDTA, 1mMEGTA, 1mMsodium orthovanadate, 50mMsodium fluoride, 0.1%2-mercaptoethanol, 1%triton X-100, plus proteases inhibitor cocktail; Sigma). Protein samples (10mg) were separated on GENE Mate express gels and transferred to PVDF membranes (Millipore, Bedford MA). The membranes were incubated with primary antibodies overnight at 4^{o}C. Antibodies used for probing western blots include those directed against NG2, PDGFRα, pSTAT3 (Santa Cruz), total STAT3 (Santa Cruz), pJAK(Santa Cruz) , pPKC (epitomics), PECAM (Santa Cruz), SMA (sigma aldrich), iNOS (gift form Dr. Stella Tsirka) GluR1 (Epitomics), GluR2 (Epitomics), GLAST (Abcam), and GLT-1 (Abcam). Proteins were detected using an enhanced chemiluminescence substrate mixture (ECL Plus, Amersham). Antibodies were used in combination with a secondary horseradish peroxidase-conjugate (Santa Cruz Biotechnologies). For immunoprecipitation, protein extracts from PFCs were prepared in RIPA buffer containing 2%Triton X-100 and 0.2% SDS. Aliquots (200µg protein extracts) were incubated overnight with primary antibodies, as indicated for each experimental condition, and 15µl of Agarose A (Santa Cruz Biotechnology). Immunocomplexes bound to agarose A were collected by centrifugation and washed twice in 500 µl RIPA buffer containing inhibitors. Precipitated proteins were analyzed by GLAST, GLT1, pSer (Santa Cruz), GLUR1 immunoblotting. Bands were detected by using HRP-conjugated secondary antibodies and developed with a chemiluminescent substrate (ECL, Amersham). Plot data are expressed in arbitrary units (a.u) after actin normalization.

D-[^{3}H]-aspartate uptake assays. The assay for uptake of D-[^{3}H]-aspartate, a non-metabolizable analog of L-glutamate, in primary cortical astrocytes has been described in detail before (Bernabe et al., 2003). Briefly, the mixed cortical primary cultures from control and ablated animals were incubated in HEPES-buffered Krebs' modified Ringer (KRH) buffer containing ^{3}H-labeled D-[aspartate] (0.4 mCi /ml, PerkinElmer, Boston, MA, USA) for 5mins at at 37^{o}C. The cells were washed with three ice-cold KRH washes and solubilized with 0.1M NaOH. For uptake assays, cortical gliosomal preparations were made using a modified method (Weller et al., 2008). Briefly,

whole PFC slices were homogenized on ice in tissue buffer (50 mM Tris, 0.3 M sucrose, pH 7.3). Cortical homogenates were incubated in KRH buffer containing ^{3}H-labeled D-[aspartate] (0.4 mCi /ml, PerkinElmer, Boston, MA, USA) for 4 min at 37 °C and promptly terminated by filtration (Whatman). Aliquots of the cell and tissue suspensions were used for protein quantification and liquid scintillation on a Beckman LS 6500 Scintillation System.

FACS. Cell suspensions were analyzed for light forward and side scatter using a FACStar plus instrument (Beckton Dickinson, Franklin Lakes, NJ). FACS-purified cels (NG2 glia [cd140a+], activated microglia [cd11b+]) plated onto poly-D-ornithine-coated plates (0.1 mg/ml) and cultured in DMEM-F12 medium (penicillin 100 units/ml, streptomycin 100 µg/ml, human apo-transferrin 50 µg/ml, biotin 10 ng/ml, Na selenite 25 nM, insulin 2.5 µg/ml, putrescine 100 µM, progesterone 20 nM. The NG2-CM media was not supplemented with growth factors except 2% FBS and collected for 2 to 3 days before cells terminally differentiated.

Primary astrocyte and neuronal cultures. Cortical astrocyte cultures were prepared as previously described (Albuquerque et al., 2009). PFCs were dissected and then mechanically dissociated by means of a fire-polished Pasteur pipette. Cells were then plated in 60 mm tissue culture dishes in DMEM high-glucose medium containing 2 mm glutamine, 5% fetal bovine serum, and 5% horse serum. Approximately 24 hr after plating, the medium was completely replaced, and the cells were grown for 10 days in vitro (DIV) with a complete medium change every 48 hr. >75% of cells in these cultures were positive for glial fibrillary acidic protein (GFAP). Hippocampal neuron cultures were prepared as previously described (Kaech and Banker, 2006)

Cell transfection and luciferase assays. Cortical astrocytes were obtained from brain cortex tissue as above. Astrocytes were plated in 12-well cell culture dishes at a density of 300 cells/µl for 24 hours. At the time of transfection, cell cultures were approximately 60% confluent. 1.5 µg of plasmid containing the firefly luciferase gene under the regulation of the 2.5-kb gfap promoter (GF1L) was transfected (Asano et al., 2009). Co-transfected TK–renilla Luciferase was used to normalize samples for transfection efficiency and for sample handling. Fresh medium or NG2CM was used 24hrs after cell transfection. Luciferase assays were performed 48hr after transfection using the Dual Assay Luciferase kit (Promega). Cell transfections were performed using the NeuroPORTER Transfection reagent (Genlantis, San Diego, CA) following manufacturer's instructions. Cells were lysed, and luciferase activity was measured following the protocol recommended by the manufacturer. Promoter activity was defined as the ratio between firefly and Renilla luciferase activities.

Biotinylation of cell surface markers. Cortical astrocyte cultures were prepared as above from the PFCs of control and iDTR mice. Cells were plated onto poly-D-ornithine-coated plates (0.1 mg/ml) and cultured in 2% DMEM-N1 medium (100 units/ml penicillin-streptomycin 100 µg/ml, human apo-transferrin 50 µg/ml, biotin 10 ng/ml, Na selenite, 25 nM, insulin 2.5 µg/ml, putrescine 100 µM, progesterone 20 nM) for 48 hours at 37°C before performing the assay. After adding fresh medium or NG2CM at different time points, astrocytes were washed twice with ice-cold PBS Ca/Mg. Cells were then incubated in 2 ml biotinylation solution (1 mg/ml NHS-biotin in PBS Ca/Mg) for

25 min at 4°C with gentle shaking. The solution was aspirated, and un-reacted biotin was quenched by incubating cells with PBS Ca/Mg containing 100 mM glycine for 25 min at 4°C with gentle agitation. Cells were lysed in 0.7 ml of radioimmunoprecipitation assay (RIPA) buffer containing protease inhibitors (1 μg/ml leupeptin, 250 μM phenylmethanesulfonyl fluoride, 1 μg/ml aprotinin, and 1 mM iodoacetamide. Cellular debris was removed by centrifugation at 17,000 × g for 20 min at 4°C, and biotinylated proteins were batch-extracted using UltraLink immobilized monomeric avidin beads. SDS-PAGE sample buffer was added to cell lysates, biotinylated proteins (cell surface proteins), and non-biotinylated proteins (intracellular proteins). These three fractions were diluted so that the sum of the immunoreactivity in the biotinylated and non-biotinylated fractions would equal that observed in the lysate if the yield from extraction were 100%. For glutamate transporter proteins present in gliosomes, biochemical measurement of intracellular and membrane-bound proteins was performed as previously described (Yuen et al., 2012). In brief, cortical slices were incubated in 1 mg/ml sulfo-*N*-hydroxysuccinimide-LC-Biotin (Pierce Chemical Co., Rockford, IL, USA) for 20 min on ice, followed by homogenization in RIPA homogenization buffer (Santa Cruz Biotechnologies). The homogenates were then incubated with 50% Neutravidin Agarose (Pierce Chemical Co.) for 2 hr at 4°C, and bound proteins were resuspended in SDS sample buffer, boiled, and processed with SDS-PAGE.

RNA isolation & cDNA synthesis Total RNA from cd140a+-sorted cells obtained from the PFCs of control, resilient and susceptible animals tissues was extracted using the RNeasy Mini Kit (Qiagen) following the manufacturer's instructions. cDNA was synthesized by RT^2 First Strand Kit (Qiagen) following the manufacturer's instructions.

BEHAVIORAL ANAYLSES

Social interaction test (S.I). Twenty-four hours after the final social defeat stress interaction, SI.I. test was performed to determine whether the animals were susceptible or resilient(Golden et al., 2011). Mice were placed into a novel arena, and their movement was monitored for 2.5 min with or without the aggressive CD1 mouse. Using the Ethovision tracking software, social interaction is calculated as a ratio of the time spent in the interaction zone with an aggressive mouse present to the time spent with the aggressive mouse absent. All mice with a ratio above 1 were classified as resilient, and all mice with a ratio below 1 were classified as susceptible.

Subthreshold social-defeat stress protocol (Microdefeat). In order to measure increased susceptibility to stress, we used a sub-threshold adaptation on the SDSP ("microdefeat") as previously described (Golden et al., 2013). Briefly, the control, 7DT and 21dpDT animals were exposed to a novel CD1 aggressor for 5 min for three consecutive times, each separated by 15 min. Twenty-four hours later, mice were assessed using the social interaction test described above.

Open Field Test. In order to measure general motor activity and anxiety-associated behavior, we used the Open Field Test (Prut and Belzung, 2003). Control and ablated animals were placed on a corner of a 40 cm^2 gridded field and monitored for 15 minutes at one day before the start of injection and at 7DT, 7dpDT and 21dpDT (Fig. 2A). The frequency of center entry was calculated as a % over overall activity.

Sucrose preference. To determine whether mice acquired anhedonic response after NG2 glia depletion in the PFC, we performed a standard sucrose preference assay as previously described (Snyder et al., 2011). Briefly, animals were habituated for 72hrs to 1% sucrose, and following a 4hrs deprivation period, then preference for sucrose (1%) or water was determined for 24hr period. Bottles were weighed the next morning. Sucrose preference was expressed as (Δweightsucrose) / (Δweightsucrose + Δweightwater) x 100.

Elevated Plus Maze. The Elevated Plus Maze for mice set-up was purchased from Noldus Information Technology. The arms were connected together by a central area, and the maze was elevated 1 m from the floor. At the beginning of the test, under controlled light conditions, mice were placed in the central area, facing one of the open arms, and the frequency of open arm entries were recorded.

Congenital Learned Helpless Rats. By selecting for susceptibility to learned helplessness, two lines of rats were generated: cLH (congenitally learned helpless) and cNLH (congenitally non-helpless). Breeding of the helplessness colonies has been described (Shumake et al., 2000). Briefly, Sprague–Dawley rats were tested in the learned helplessness paradigm (Shumake et al., 2000). Twenty-four hours after a total of 20 min uncontrollable and unpredictable 0.8 mA footshocks, the rats were tested in an escape paradigm where foot shock could be eliminated with a single lever press: animals with more than 10 failures (out of 15 trials) to eliminate footshock were considered as helpless, animals with less than five failures were considered as non-helpless. Helpless animals and non-helpless animals, respectively, were mated for the subsequent generations avoiding sib crosses and resulting in two selective strains: the congenitally helpless strain (cLH), demonstrating helpless behavior without prior inescapable shock, and the congenitally non-helpless strain (cNLH), resistant to the development of learned helplessness.

Confocal microscopy, cell counting and statistical analyses. A confocal laser-scanning microscope TCS-SP5 (Leica DMI6000 B instrument) was used for image localization of FITC (488-nm laser line excitation; 522/35 emission filter), CY3 (570-nm excitation; 605/32 emission filter) and Cy5 (647 excitation; 680/32 emission filter). Optical sections (z = 0.5 μm) of confocal epifluorescence images were sequentially acquired using a 63× objective (NA = 1.40), with LAS AF software. NIH ImageJ software was then used to merge images. Merged images were processed in Photoshop Cs4 software with minimal manipulations of contrast. At least four different brains for each strain and each experimental condition were analyzed and counted. Cell counting was performed blindly, and tissue sections were matched across samples. An average of 15–20 sections were quantified using unbiased stereological morphometric analysis to obtain an estimate of the total number of positive cells. All cell quantification data were obtained by cell counting using ImageJ, and data are presented as the mean cell number per cubic millimeter (x1000). Statistical tests used per experiment are indicated in the figure legends. Statistical analyses were perfomed using SigmaPlot10.

Supplemental References

Albuquerque, C., Joseph, D.J., Choudhury, P., and MacDermott, A.B. (2009). Dissection, plating, and maintenance of cortical astrocyte cultures. Cold Spring Harb Protoc *2009*, pdb prot5273.

Asano, H., Aonuma, M., Sanosaka, T., Kohyama, J., Namihira, M., and Nakashima, K. (2009). Astrocyte differentiation of neural precursor cells is enhanced by retinoic acid through a change in epigenetic modification. Stem cells *27*, 2744-2752.

Bernabe, A., Mendez, J.A., Hernandez-Kelly, L.C., and Ortega, A. (2003). Regulation of the Na+-dependent glutamate/aspartate transporter in rodent cerebellar astrocytes. Neurochem Res *28*, 1843-1849.

Golden, S.A., Christoffel, D.J., Heshmati, M., Hodes, G.E., Magida, J., Davis, K., Cahill, M.E., Dias, C., Ribeiro, E., Ables, J.L*., et al.* (2013). Epigenetic regulation of RAC1 induces synaptic remodeling in stress disorders and depression. Nature medicine *19*, 337-344.

Golden, S.A., Covington, H.E., 3rd, Berton, O., and Russo, S.J. (2011). A standardized protocol for repeated social defeat stress in mice. Nat Protoc *6*, 1183-1191.

Kaech, S., and Banker, G. (2006). Culturing hippocampal neurons. Nat Protoc *1*, 2406-2415.

Prut, L., and Belzung, C. (2003). The open field as a paradigm to measure the effects of drugs on anxiety-like behaviors: a review. Eur J Pharmacol *463*, 3-33.

Shumake, J., Poremba, A., Edwards, E., and Gonzalez-Lima, F. (2000). Congenital helpless rats as a genetic model for cortex metabolism in depression. Neuroreport *11*, 3793-3798.

Snyder, J.S., Soumier, A., Brewer, M., Pickel, J., and Cameron, H.A. (2011). Adult hippocampal neurogenesis buffers stress responses and depressive behaviour. Nature *476*, 458-461.

Weller, M.L., Stone, I.M., Goss, A., Rau, T., Rova, C., and Poulsen, D.J. (2008). Selective overexpression of excitatory amino acid transporter 2 (EAAT2) in astrocytes enhances neuroprotection from moderate but not severe hypoxia-ischemia. Neuroscience *155*, 1204-1211.

Yuen, E.Y., Wei, J., Liu, W., Zhong, P., Li, X., and Yan, Z. (2012). Repeated stress causes cognitive impairment by suppressing glutamate receptor expression and function in prefrontal cortex. Neuron *73*, 962-977.

References for Figure 8C

A. Turner, C. A., Akil, H., Watson, S. J. & Evans, S. J. The fibroblast growth factor system and mood disorders. Biological psychiatry **59**, 1128-1135, doi:10.1016/j.biopsych.2006.02.026 (2006).

B. Turner, C. A., Calvo, N., Frost, D. O., Akil, H. & Watson, S. J. The fibroblast growth factor system is downregulated following social defeat. Neuroscience letters **430**, 147-150,

C. Turner, C. A., Gula, E. L., Taylor, L. P., Watson, S. J. & Akil, H. Antidepressant-like effects of intracerebroventricular FGF2 in rats. Brain research **1224**, 63-68,

D. Turner, C. A., Watson, S. J. & Akil, H. Fibroblast growth factor-2: an endogenous antidepressant and anxiolytic molecule? Biological psychiatry **72**, 254-255, doi:10.1016/j.biopsych.2012.05.025 (2012).

E. Elsayed, M. et al. Antidepressant effects of fibroblast growth factor-2 in behavioral and cellular models of depression. Biological psychiatry **72**, 258-265, doi:10.1016/j.biopsych.2012.03.003 (2012).

F. Turner, C. A., Watson, S. J. & Akil, H. The fibroblast growth factor family: neuromodulation of affective behavior. Neuron **76**, 160-174, doi:10.1016/j.neuron.2012.08.037 (2012)

G. Suzuki, K. et al. Transient upregulation of the glial glutamate transporter GLAST in response to fibroblast growth factor, insulin-like growth factor and epidermal growth factor in cultured astrocytes. Journal of cell science **114**, 3717-3725 (2001).

H. Chew, L. J. et al. Growth factor-induced transcription of GluR1 increases functional AMPA receptor density in glial progenitor cells. The Journal of neuroscience : the official journal of the Society for Neuroscience **17**, 227-240 (1997).

I. Cheng, B. et al. Basic fibroblast growth factor selectively increases AMPA-receptor subunit GluR1 protein level and differentially modulates Ca2+ responses to AMPA and NMDA in hippocampal neurons. Journal of neurochemistry **65**, 2525-2536 (1995)

J. de Azevedo Cardoso, T. et al. Neurotrophic factors, clinical features and gender differences in depression. Neurochemical research **39**, 1571-1578, doi:10.1007/s11064-014-1349-4 (2014).

K. Liu, X. et al. Elevated serum levels of FGF-2, NGF and IGF-1 in patients with manic episode of bipolar disorder. Psychiatry research **218**, 54-60, doi:10.1016/j.psychres.2014.03.042 (2014).

L. Banerjee, R., Ghosh, A. K., Ghosh, B., Bhattacharyya, S. & Mondal, A. C. Decreased mRNA and Protein Expression of BDNF, NGF, and their Receptors in the Hippocampus from Suicide: An Analysis in Human Postmortem Brain. Clinical medicine insights. Pathology **6**, 1-11, doi:10.4137/CMPath.S12530 (2013).

M. Bilgen, A. E. et al. Effects of electroconvulsive therapy on serum levels of brain-derived neurotrophic factor and nerve growth factor in treatment resistant major depression. Brain research bulletin **104**, 82-87, doi:10.1016/j.brainresbull.2014.04.005 (2014).

N. Cirillo, G. et al. Reactive astrocytosis-induced perturbation of synaptic homeostasis is restored by nerve growth factor. Neurobiology of disease **41**, 630-639, doi:10.1016/j.nbd.2010.11.012 (2011).

O. Levi-Montalcini, R. The nerve growth factor 35 years later. Science **237**, 1154-1162 (1987).

P. Barbosa, I. G. et al. Decreased plasma neurotrophin-4/5 levels in bipolar disorder patients in mania. Revista brasileira de psiquiatria **0**, 0 (2014).

Q. DeFazio, R. A., Pong, K., Knusel, B. & Walsh, J. P. Neurotrophin-4/5 promotes dendritic outgrowth and calcium currents in cultured mesencephalic dopamine neurons. Neuroscience **99**, 297-304 (2000).

R. Tan, H., Cao, J., Zhang, J. & Zuo, Z. Critical role of inflammatory cytokines in impairing biochemical processes for learning and memory after surgery in rats. Journal of neuroinflammation **11**, 93, doi:10.1186/1742-2094-11-93 (2014).

S. Oglodek, E. A., Szota, A., Just, M. J., Mos, D. & Araszkiewicz, A. Comparison of chemokines (CCL-5 and SDF-1), chemokine receptors (CCR-5 and CXCR-4) and IL-6 levels in patients with different severities of depression. Pharmacological reports : PR **66**, 920-926

T. Milbrandt, J. et al. Persephin, a novel neurotrophic factor related to GDNF and neurturin. Neuron **20**, 245-253 (1998).